Phys Chem Minerals (2003) 30: 409–415
DOI 10.1007/s00269-003-0332-4


ORIGINAL PAPER

H. Kojitani · K. Nishimura · A. Kubo · M. Sakashita
K. Aoki · M. Akaogi

# Raman spectroscopy and heat capacity measurement of calcium ferrite type $MgAl_2O_4$ and $CaAl_2O_4$

Received: 4 November 2002 / Accepted: 29 April 2003

**Abstract** Raman spectroscopy of calcium ferrite type $MgAl_2O_4$ and $CaAl_2O_4$ and heat capacity measurement of $CaAl_2O_4$ calcium ferrite were performed. The heat-capacity of $CaAl_2O_4$ calcium ferrite measured by a differential scanning calorimeter (DSC) was represented as $C_P(T) = 190.6–1.116 \times 10^7 T^{-2} + 1.491 \times 10^9 T^{-3}$ above 250 K ($T$ in K). The obtained Raman spectra were applied to lattice dynamics calculation of heat capacity using the Kieffer model. The calculated heat capacity for $CaAl_2O_4$ calcium ferrite showed good agreement with that by the DSC measurement. A Kieffer model calculation for $MgAl_2O_4$ calcium ferrite similar to that for $CaAl_2O_4$ calcium ferrite was made to estimate the heat capacity of the former. The heat capacity of $MgAl_2O_4$ calcium ferrite was represented as $C_P(T) = 223.4–1352T^{-0.5} - 4.181 \times 10^6 T^{-2} + 4.300 \times 10^8 T^{-3}$ above 250 K. The calculation also gave approximated vibrational entropies at 298 K of calcium ferrite type $MgAl_2O_4$ and $CaAl_2O_4$ as 97.6 and 114.9 J mol$^{-1}$ K$^{-1}$, respectively.

**Keywords** Calcium ferrite · Heat capacity · Differencial scanning calorimetry · Raman · Kieffer model

H. Kojitani (✉) · K. Nishimura · A. Kubo · M. Akaogi
Department of Chemistry, Faculty of Science,
Gakushuin University, 1-5-1 Mejiro,
Toshima-ku, Tokyo 171-8588, Japan
e-mail: hiroshi.kojitani@gakushuin.ac.jp
Fax: +81-3-5992-1029

K. Aoki · M. Sakashita
National Institute of Advanced Industrial Science
and Technology (AIST), Tsukuba Central 5,
1-1-1 Higashi, Tsukuba, Ibaraki 305-8565, Japan

*Present address*: A. Kubo
Institue for Study of the Earth's Interior,
Okayama University, 827 Yamada, Misasa,
Tottori 682-0193, Japan

*Present address*: K. Aoki
Synchrotron Radiation Research Center, Kansai Research
Establishment, Japan Atomic Energy Research Institute,
Kouto 1-1-1, Mikazuki-cho, Sayo-gun, Hyogo 679-5148, Japan

## Introduction

Recent high-pressure and high-temperature experiments have reported the presence of Al-rich phases in high-pressure phases of mid-ocean ridge basalt (MORB) under lower mantle conditions (e.g. Irifune and Ringwood 1993; Kesson et al. 1994; Hirose et al.1999; Ono et al. 2001). In particular, a calcium ferrite-type phase is expected as a possible host of Al and alkali elements in the lower mantle (Kesson et al. 1994; Akaogi et al. 1999). According to observation on high-pressure phase assemblages of MORB by Miyajima et al. (2001), the composition of the calcium ferrite shows that $MgAl_2O_4$ and $CaAl_2O_4$ are among the major components containing divalent cations. To clarify the stability of the calcium ferrite phases at high pressure and high temperature, their thermochemical properties are needed, but they have not yet been reported.

Generally, in high-pressure materials, a small amount of sample insufficient for calorimetry or the instability of a sample under ambient conditions makes direct thermochemical measurement difficult. Even in such materials, however, heat capacity, entropy and Debye temperature can be estimated by a calculation based on lattice dynamics of crystal, when the phonon dispersion property of the lattice vibration is known. Raman and infrared spectra give us very useful information on lattice vibration which is needed in the calculation.

In this study, Raman spectra of calcium ferrite type $MgAl_2O_4$ and $CaAl_2O_4$ and heat capacity at constant pressure ($C_P$) of $CaAl_2O_4$ calcium ferrite were measured. The obtained Raman spectra were applied to the calculation of $C_P$ by the Kieffer model (Kieffer 1979a). The measured $C_P$ of $CaAl_2O_4$ calcium ferrite was compared with that by calculation to assess the calculated $C_P$. Because of the difficult synthesis of a sufficient amount of $MgAl_2O_4$ calcium ferrite for $C_P$ measurement, the $C_P$ of $MgAl_2O_4$ calcium ferrite was estimated by the Kieffer model calculation using a model for phonon density of state similar to that of $CaAl_2O_4$

calcium ferrite. Entropies and thermal Debye temperatures of calcium ferrite type $MgAl_2O_4$ and $CaAl_2O_4$ are calculated from the heat capacities. A Clapeyron slope of the boundary of formation of $MgAl_2O_4$ calcium ferrite from $Al_2O_3$ + MgO is also discussed.

## Experimental

### Sample syntheses

$MgAl_2O_4$ spinel was used as a starting material for high-pressure synthesis of $MgAl_2O_4$ calcium ferrite. The $MgAl_2O_4$ spinel was prepared by heating a stoichiometric mixture of reagent grade MgO and $\alpha$-$Al_2O_3$ at 1773 K for 24 h. A Kawai-type multianvil high-pressure apparatus at Gakushuin University was used for synthesizing $MgAl_2O_4$ calcium ferrite. The truncated edge length (TEL) of tungsten carbide anvils was 1.5 mm. The high-pressure cell assembly used in the synthesis was the same as that in Kubo and Akaogi (2000). The starting material was kept at 27 GPa and about 2273 K for 8 min, then quenched, and the run product was recovered to ambient conditions. $CaAl_2O_4$ calcium ferrite was synthesized by a procedure similar to that of $MgAl_2O_4$ calcium ferrite. The starting compound for $CaAl_2O_4$ calcium ferrite synthesis was $CaAl_2O_4$-stuffed tridymite, which was made by heating a stoichiometric mixture of reagent grade $CaCO_3$ and $\alpha$-$Al_2O_3$ at 1623 K for 10 days (Akaogi et al. 1999). Tungsten carbide anvils with TEL of 5 mm were used for the high-pressure syntheses. The $CaAl_2O_4$-stuffed tridymite was kept at 15 GPa and 1873 K for 1 h to synthesize the calcium ferrite sample for Raman spectroscopy, and at 10 GPa and 1773 K for 1 h for heat capacity measurement samples.

The recovered samples for Raman spectroscopy were fixed on a glass slide with epoxy glue and polished by corundum-coated polishing films (grain size 1 μm). The recovered samples for heat capacity measurement were crushed to powder. These samples were identified by using powder and microfocus X-ray diffractometers at Gakushuin University (Rigaku RINT-2500V, Cr K$\alpha$, 45 kV, 250 mA). In the microfocus X-ray diffraction (XRD) method, the X-ray beam was collimated to 50 μm in diameter.

The microfocus XRD pattern of the recovered $MgAl_2O_4$ sample indicated that three phases were presented along the temperature gradient in the cylindrical sample. The sample edge area at the lowest temperature was identified as periclase + corundum. It was confirmed that the middle area consisted of an $MgAl_2O_4$ calcium ferrite phase based on XRD data by Irifune et al. (1991). An XRD pattern from the center area indicated an unknown phase.

Both microfocus and powder XRD patterns of the recovered $CaAl_2O_4$ sample showed good agreement with that of $CaAl_2O_4$ calcium ferrite reported by Akaogi et al. (1999). No other phase was detected in the recovered samples. Although the synthesis conditions were different between the calorimetric sample and the Raman sample, the XRD patterens indicated no difference between them.

### Raman spectroscopy

Raman spectra were obtained on the well-polished surfaces of polycrystalline samples by using a micro-Raman spectroscopy system at National Institute of Advanced Industrial Science and Technology (AIST) with the 514.5 nm line of an argon ion laser, SPEX triple monochromator and CCD detector. The laser power at the sample surface was approximately 5 mW to avoid overheating the high-pressure materials and to decrease the effect of fluorescence. The laser beam diameter was 5–10 μm. Raman data were collected by repeated exposures of 60 s five times for each measurement of $MgAl_2O_4$ and $CaAl_2O_4$. A super notch filter was used in the measurement of the lower wavenumber region. The wavenumber of the Raman shift was calibrated with an Ne lamp. For the Raman peak analysis, the software Peak Fit (SPSS Inc.) was used for profile fitting.

### Heat capacity measurement

The heat capacity at constant pressure ($C_P$) of $CaAl_2O_4$ calcium ferrite was measured using a heat flux-type differential scanning calorimeter (DSC, Rigaku-DSC8230B) in the temperature range from 150 to 730 K. A detailed procedure is given in Akaogi et al. (1990). A powdered sample (23.68 mg) was packed in a tightly crimped aluminum pan. A reagent-grade $\alpha$-$Al_2O_3$ powder (23.42 mg) was used as the heat capacity standard. The sample and the standard were run alternately. $C_P$ measurements were performed in two temperature ranges; 155–350 K and 353–733 K. In the high-temperature range run, data were collected with a constant heating rate of 7 K $min^{-1}$ at 10 K intervals. In the low-temperature run, the calorimetric chamber was cooled first by liquid nitrogen, and then the measurements were made with a heating rate of 6 K $min^{-1}$ at 5 K intervals under Ar gas flow at the rate of 5 $cm^3$ $min^{-1}$ to prevent condensation of water in air. The $C_P$ measurements were repeated 21 times in the high-temperature range and 13 times in the low-temperature range, and the data were averaged at each temperature. Powder XRD showed no change in the sample after the series of heat capacity measurements.

## Results and discussion

### Raman spectra of calcium ferrite type $MgAl_2O_4$ and $CaAl_2O_4$

Typical Raman spectra of calcium ferrite type $MgAl_2O_4$ and $CaAl_2O_4$ are shown in Fig. 1a and b, respectively. In the crystal structure of calcium ferrite, double chains which consist of edge-shared $AlO_6$ polyhedra extend along the *c*-axis direction, and four double chains form a tunnel where divalent cations are placed. The divalent cation site has eight-coordination of oxygens and can accommodate an ion which has a relatively large ion radius (Reid et al. 1968; Reid and Ringwood 1969). The symmetry of the structure belongs to the orthorhombic space group *Pbnm*. The irreducible representation is:

$$\Gamma = 14A_g + 14B_{1g} + 7B_{2g} + 7B_{3g} + 7A_u + 7B_{1u} + 14B_{2u} + 14B_{3u} \quad . \qquad (1)$$

Raman-active modes among them are $14A_g$ + $14B_{1g}$ + $7B_{2g}$ + $7B_{3g}$. The observed Raman shifts for both calcium ferrites are tabulated in Table 1. The Raman shifts were determined within the uncertainty of 2–3 $cm^{-1}$. Although a total of 42 Raman peaks are expected, the number of observed peaks for both the samples is less than 42. In both the Raman spectra, most peaks distribute between 150 and 800 $cm^{-1}$. Some residual peaks are observed in the range between 800 and 1200 $cm^{-1}$. A qualitative lattice vibrational calculation using the WMIN program (Busing 1981) with the CMAS94 potential (Matsui 1994) implies that peaks lower than about 250 $cm^{-1}$ are generally attributed to translational modes of $Mg^{2+}$ or $Ca^{2+}$ and that peaks between 250 and 550 $cm^{-1}$ are due to rotational modes of $AlO_6$ polyhedra and translational modes of $Al^{3+}$. The calculation also suggests that peaks higher than about 550 $cm^{-1}$ are caused by stretching modes of $AlO_6$.

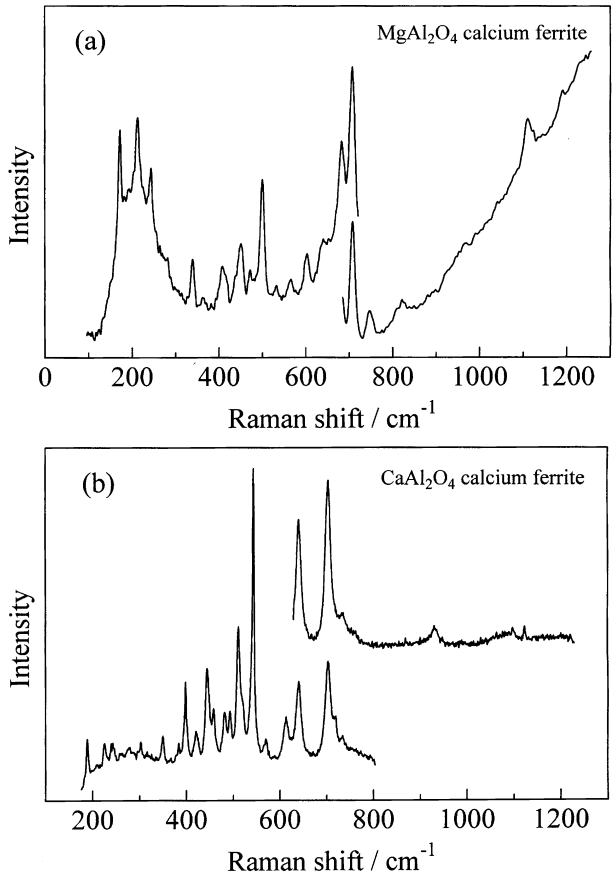


**Fig. 1a, b** Raman spectra of **a** $MgAl_2O_4$ calcium ferrite and **b** $CaAl_2O_4$ calcium ferrite

An intense peak at 707 $cm^{-1}$ and an asymmetric one at 1123 $cm^{-1}$ are observed in the spectrum of $MgAl_2O_4$ calcium ferrite, and similar peaks are also observed in the spectrum of $CaAl_2O_4$ calcium ferrite at almost the same positions. These peaks might be assigned to the stretching mode of $AlO_6$ polyhedra which are substructures in both the calcium ferrite type $MgAl_2O_4$ and $CaAl_2O_4$. Several peaks around 200 $cm^{-1}$ of the $MgAl_2O_4$ calcium ferrite spectrum seem to be located at slightly lower frequencies than those in $CaAl_2O_4$ calcium ferrite. This observation is consistent with the interpretation that the ionic radius of $Mg^{2+}$, smaller than that of $Ca^{2+}$, results in a weaker bonding force of Mg–O in the large divalent cation site, which causes a lower vibrational frequency than that of Ca–O.

## Measured heat capacity of $CaAl_2O_4$ calcium ferrite

The result of $C_P$ measurement of $CaAl_2O_4$ calcium ferrite is shown in Table 2 and Fig. 2. Although the uncertainty of the data generally increases with increasing temperature, the relative error is about 2%. The heat capacities measured in two different temperature ranges show good agreement within the errors around 350 K. The $C_P$ data in the range of 250–733 K were fitted to the Berman and Brown $C_P$ equation (Berman and Brown 1985) by the least-squares method. The resultant coefficients of the $C_P$ equation are given in Table 3.

**Table 1** Observed Raman peaks of calcium ferrite type $MgAl_2O_4$ and $CaAl_2O_4$

| Raman shift/$cm^{-1}$ | |
|---|---|
| $MgAl_2O_4$ | $CaAl_2O_4$ |
| 173 | 175–178 |
| 192–195 | 188–189 |
| 202–206 | 197–199 |
| 214–215 | 225–227 |
| 236–239 | 229–232 |
| 243–244 | 233–237 |
| 253–256 | 242–243 |
| 282 | 256–259 |
| 339–340 | 272–274 |
| 354–357 | 277–279 |
| 362–364 | 284–286 |
| 379–382 | 301–303 |
| 391–395 | 350–351 |
| 406–409 | 383–385 |
| 416–419 | 398–399 |
| 433–437 | 420–422 |
| 449–451 | 444–446 |
| 470–471 | 458–459 |
| 485–487 | 482–483 |
| 499–500 | 494–495 |
| 525–531 | 511–512 |
| 564–567 | 521–522 |
| 574–577 | 542–543 |
| 588–595 | 570–571 |
| 601–602 | 613–614 |
| 637–640 | 640–642 |
| 646–654 | 703–704 |
| 680–682 | 716–720 |
| 707–708 | 734–736 |
| 742–745 | 758–760 |
| 820–821 | 930–931 |
| 1106–1109 | 1082–1089 |
| 1122—1124 | 1090–1091 |
| 1190—1193 | 1123–1124 |

## Kieffer model calculation of heat capacity

The Kieffer model gives a good approximation of heat capacity and entropy in spite of rather simplified density of state for phonon dispersion. Therefore, it has been applied to many silicates and oxides (e.g. Kieffer 1979c, 1980; Akaogi et al. 1984; Ross et al. 1986; Hofmeister 1987). In the model, heat capacity at constant volume ($C_V$) is calculated by modelling a simplified phonon density of state of a crystal, by elastic constants for acoustic modes and based on Raman and IR spectra for optic modes (Kieffer 1979a,b,c). The $C_P$ is calculated using the following relation:

$$C_P = C_V + \alpha^2 K_T V T, \quad (2)$$

where $\alpha$, $K_T$ and $V$ refer to thermal expansivity, isothermal bulk modulus and volume, respectively. We calculated heat capacities and entropies of calcium ferrite type $MgAl_2O_4$ and $CaAl_2O_4$ using the Kieffer model. Detailed calculation procedures are described below.

**Table 2** The result of heat capacity measurement of $CaAl_2O_4$ calcium ferrite

| $T$/K | $C_P$/J mol$^{-1}$ K$^{-1}$ |
|---|---|
| 155 | 60.1 ± 2.1 |
| 160 | 63.0 ± 2.6 |
| 165 | 64.9 ± 2.1 |
| 170 | 67.9 ± 1.9 |
| 175 | 71.6 ± 1.9 |
| 180 | 74.5 ± 1.7 |
| 185 | 76.1 ± 1.9 |
| 190 | 79.4 ± 1.8 |
| 195 | 82.0 ± 1.7 |
| 200 | 85.3 ± 1.9 |
| 205 | 86.2 ± 1.6 |
| 210 | 88.7 ± 2.5 |
| 215 | 91.4 ± 1.7 |
| 220 | 93.6 ± 1.5 |
| 225 | 96.3 ± 1.8 |
| 230 | 98.7 ± 1.9 |
| 235 | 100.9 ± 2.1 |
| 240 | 102.8 ± 2.1 |
| 245 | 104.3 ± 2.0 |
| 250 | 107.4 ± 2.7 |
| 255 | 109.4 ± 2.8 |
| 260 | 112.1 ± 3.8 |
| 265 | 111.7 ± 2.9 |
| 270 | 112.3 ± 2.7 |
| 275 | 113.9 ± 1.4 |
| 280 | 115.4 ± 1.5 |
| 285 | 116.3 ± 1.1 |
| 290 | 117.0 ± 1.8 |
| 295 | 120.5 ± 1.8 |
| 300 | 123.2 ± 2.0 |
| 305 | 124.4 ± 2.5 |
| 310 | 127.1 ± 3.8 |
| 315 | 126.7 ± 3.0 |
| 320 | 128.6 ± 3.4 |
| 325 | 127.8 ± 2.1 |
| 330 | 129.3 ± 1.0 |
| 335 | 129.4 ± 1.6 |
| 340 | 131.7 ± 1.8 |
| 345 | 132.3 ± 1.7 |
| 350 | 132.1 + 2.0 |
| 353 | 134.6 ± 1.8 |
| 363 | 137.9 ± 1.3 |
| 373 | 140.1 ± 1.8 |
| 383 | 142.5 ± 1.6 |
| 393 | 143.3 ± 1.4 |
| 403 | 144.5 ± 1.5 |
| 413 | 144.3 ± 1.6 |
| 423 | 146.3 ± 2.2 |
| 433 | 146.3 ± 2.1 |
| 443 | 151.5 ± 2.1 |
| 453 | 152.8 ± 1.2 |
| 463 | 154.3 ± 1.4 |
| 473 | 154.5 ± 1.4 |
| 483 | 156.4 ± 1.8 |
| 493 | 156.2 ± 1.4 |
| 503 | 158.7 ± 1.6 |
| 513 | 159.3 ± 1.6 |
| 523 | 160.7 ± 1.9 |
| 533 | 162.2 ± 2.8 |
| 543 | 163.2 ± 2.5 |
| 553 | 164.5 ± 1.8 |
| 563 | 164.3 ± 1.8 |
| 573 | 164.9 ± 1.6 |
| 583 | 164.9 ± 1.7 |
| 593 | 168.7 ± 2.3 |
| 603 | 167.8 ± 2.6 |
| 613 | 168.9 ± 2.1 |
| 623 | 169.1 ± 2.4 |
| 633 | 168.2 ± 3.0 |
| 643 | 168.2 ± 2.5 |
| 653 | 170.5 ± 2.6 |
| 663 | 169.9 ± 2.1 |
| 673 | 170.9 ± 2.1 |
| 683 | 170.3 ± 2.3 |
| 693 | 170.6 ± 2.0 |
| 703 | 171.5 ± 1.9 |
| 713 | 172.3 ± 2.2 |
| 723 | 172.2 ± 2.8 |
| 733 | 171.7 ± 5.3 |

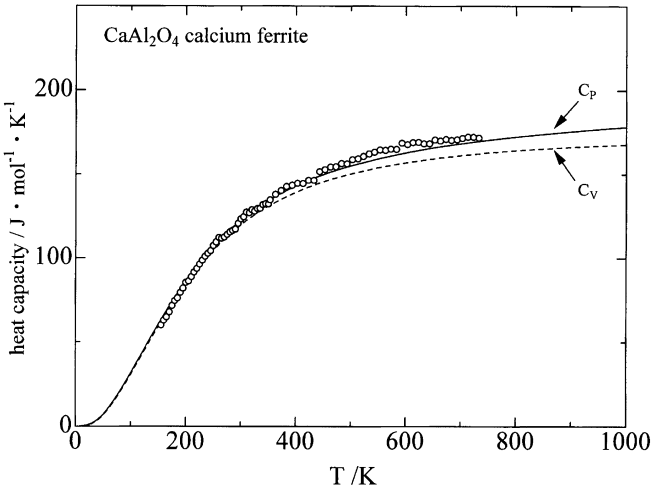


**Fig. 2** Measured and calculated heat capacities of $CaAl_2O_4$ calcium ferrite. *Open circles* show measured heat capacity. *Solid and dashed curves* represent heat capacity at constant pressure ($C_P$) and heat capacity at constant volume ($C_V$), respectively, calculated by the Kieffer model

In the Kieffer model calculation, the acoustic and optic modes were modelled as follows. To approximate the contribution of acoustic modes to heat capacity, directionally averaged sound velocities, $u_1$, $u_2$ and $u_3$, are used; $u_1$ and $u_2$ are slower and faster transverse wave velocities, respectively, and $u_3$ is a longitudinal wave velocity. They were derived from elastic wave speeds, $v_P$ and $v_S$. The $v_P$, i.e. $u_3$, was calculated from the empirical relationship based on Birch (1961); $v_P = -1.87 - 0.7 \times (m-21) + 3.05\rho$, where $\rho$ and $m$ refer to density and mean atomic weight, respectively. Although the $v_P$ values of crystals and rocks shown in Birch (1961) were measured at 1 GPa, the equation is useful to estimate a $v_P$ at ambient pressure because, for example, the difference between density of $MgAl_2O_4$ calcium ferrite at ambient pressure and that at 1 GPa is very small (0.2%). $v_S$ was obtained by the equation; $v_S = [3/4(v_P{}^2 - K_S/\rho)]^{1/2}$, where $K_S$ is adiabatic bulk modulus and assumed to be equal to isothermal bulk modulus, $K_T$. As bulk modulus of $CaAl_2O_4$ calcium ferrite has not yet been measured; it was estimated from the relationship by Anderson and

**Table 3** Berman and Brown's $C_P$ equation for calcium ferrite type $CaAl_2O_4$ and $MgAl_2O_4$

$C_P^\circ = k_1 + k_2T^{-0.5} + k_3T^{-2} + k_4T^{-3}$ [a] (J mol$^{-1}$ K$^{-1}$)

| | $CaAl_2O_4$ [b] | $MgAl_2O_4$ [c] |
|---|---|---|
| $k_1 \times 10^{-2}$ | 1.906 | 2.234 |
| $k_2 \times 10^{-3}$ | 0 | −1.352 |
| $k_3 \times 10^{-7}$ | −1.116 | −0.4181 |
| $k_4 \times 10^{-9}$ | 1.491 | 0.4300 |

[a] $T$ in K
[b] Calorimetric $C_P$ data from 250 to 730 K were fitted by the least squares method
[c] Calculated $C_P$ from 250 to 1500 K by the Kieffer model were used for the least-squares fitting

Anderson (1970): $[K_T \times V]_x = C_x$, where $V$ and $x$ refer to molar volume and a given crystal structure, respectively, and $C_x$ is a constant characteristic of the structure $x$. $u_1$ and $u_2$ were calculated using the Eqs. (A3) and (A7) in Kieffer (1979a). Since the minimum of $v_s$ referred to $v_{\min,S}$ was needed in the calculation, the $v_{\min,S}$ was obtained by adopting the averaged $v_{\min,S}/v_{VRH,S}$ ratio of 0.81 ± 0.06 from 13 data (coesite data was excluded because of the large deviation) in Table A1 in Kieffer (1979a), where $v_{VRH,S}$ is assumed to be the same as $v_S$. Models of optic modes were determined based on the obtained Raman spectra. In the model for $CaAl_2O_4$ calcium ferrite, the Raman peak group from 175 to 760 cm$^{-1}$ was represented as one optic continuum and Raman peaks higher than about 900 cm$^{-1}$ were expressed by another optic continuum. This optic mode model is illustrated in Fig. 3. The parameters used in the Kieffer model calculations are summarized in Table 4.

The calculated $C_P$ of $CaAl_2O_4$ calcium ferrite by the Kieffer model shows very good agreement with the observed one (Fig. 2) in spite of a simple optic continua model. When the approximated $v_{\min,S}/v_{VRH,S}$ ratio is changed within the uncertainty, the differences in calculated $C_P$ value at a given temperature are negligibly small (< 0.03%). The calculated $C_P$ was varied by only 0.5% at most with a 10% change of bulk modulus. The $\alpha$ used in the calculation was assumed to be the same as that of $CaFe_2O_4$ calcium ferrite by Skinner (1966). The uncertainty in the $\alpha$ has a considerable effect on the calculated $C_P$. As many oxides and silicates have $\alpha$ in the range between $2 \times 10^{-5}$ K$^{-1}$ and $4 \times 10^{-5}$ K$^{-1}$, the effect of $\alpha$ on calculated $C_P$ was examined by varying $\alpha$ within this range. If $\alpha = 2.0 \times 10^{-5}$ K$^{-1}$ is used instead of $3.2 \times 10^{-5}$ K$^{-1}$, calculated $C_P$ at 1500 K is 6% smaller than that by $3.2 \times 10^{-5}$ K$^{-1}$. When $\alpha = 4.0 \times 10^{-5}$ K$^{-1}$ is used, calculated $C_P$ at 1500 K increases by 5%. However the calculated $C_P$ with thermal expansion of $4.0 \times 10^{-5}$ K$^{-1}$ seems to be much more consistent with the observed one, especially in the temperature range higher than 300 K. The result may suggest that the $\alpha$ of $CaAl_2O_4$ calcium ferrite is probably larger than $3.2 \times 10^{-5}$ K$^{-1}$, which was used in the calculation in Fig. 2. On the other hand, $\alpha$ and $K_T$ hardly affect both

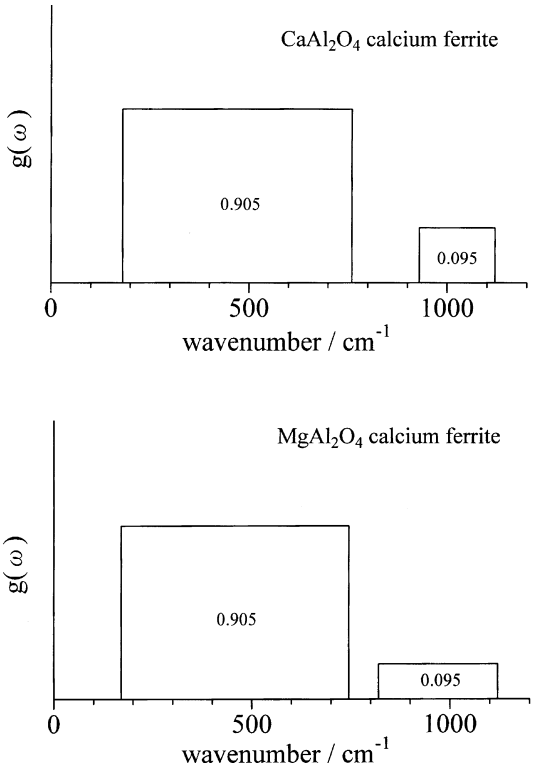


**Fig. 3** Optic continua models used for heat-capacity calculations of calcium ferrite type $MgAl_2O_4$ and $CaAl_2O_4$. *Number in each optic continuum box* refers to its density ratio

$C_P$ and $C_V$ curves below about 300 K, because they contribute mostly to the anharmonic term. The heat capacity at $T < 300$ K depends largely on a lower cutoff frequency of the first optic continuum. The good agreement between the calculated and observed $C_P$ below 300 K suggests that the present model is appropriate, though it was based on Raman data only.

Since the $C_P$ calculation for $CaAl_2O_4$ calcium ferrite by the Kieffer model gave the successful result, a similar model with two optic continua represented in Fig. 3 was adopted to calculate the $C_P$ of $MgAl_2O_4$ calcium ferrite. The parameters used in the calculation are shown in Table 4; the result of the calculation is shown in Fig. 4. The obtained $C_P$ of $MgAl_2O_4$ calcium ferrite is slightly smaller than that of $CaAl_2O_4$ calcium ferrite at a temperature below about 1000 K. The calculated $C_P$ has some uncertainty due to the undetermined $\alpha$ of $MgAl_2O_4$ calcium ferrite. The calculation using $\alpha = 2 \times 10^{-5}$ K$^{-1}$ and $4 \times 10^{-5}$ K$^{-1}$ results in about 5% smaller and about 5% larger $C_P$ at 1500 K, respectively, than that calculated with $\alpha = 3.2 \times 10^{-5}$ K$^{-1}$ adopted in this study. Coefficients of Berman and Brown's $C_P$ equation for $MgAl_2O_4$ calcium ferrite are presented in Table 3. Because uncertainties in the estimated parameters for the Kieffer model calculation do not greatly influence the $C_P$ curve at temperatures lower than 300 K, as described above, we calculated vibrational entropy at 298 K from the calculated $C_P$. The obtained entropies of calcium ferrite type $MgAl_2O_4$ and $CaAl_2O_4$ are given in

**Table 4** Physical properties used for the Kieffer model calculations $u_1$, $u_2$, $u_3$ directionally averaged acoustic velocities; $\omega_l$ lower cutoff of optic continuum; $\omega_u$ upper cutoff of optic continuum; $V_0$ unit cell volume at ambient conditions; $K_T$ isothermal bulk modulus; $\alpha$ thermal expansivity

| | $MgAl_2O_4$ | $CaAl_2O_4$ |
|---|---|---|
| $u_1$ km$^{-1}$ s$^{-1}$ | 5.49[a] | 4.12[a] |
| $u_2$ km$^{-1}$ s$^{-1}$ | 7.53[a] | 5.67[a] |
| $u_3$ km$^{-1}$ s$^{-1}$ | 10.65[a] | 9.16[a] |
| First optic continuum | | |
| $\omega_l$ cm$^{-1}$ | 170[b] | 180[b] |
| $\omega_u$ cm$^{-1}$ | 745[b] | 760[b] |
| Fraction | 0.905 | 0.905 |
| Second optic continuum | | |
| $\omega_l$ cm$^{-1}$ | 820[b] | 930[b] |
| $\omega_u$ cm$^{-1}$ | 1120[b] | 1120[b] |
| Fraction | 0.095[b] | 0.095[b] |
| Formula weight g$^{-1}$ | 142.27 | 158.04 |
| $V_0$ Å$^3$ | 239.97[c] | 264.09[d] |
| $K_T$/GPa | 241[e] | 219[a] |
| $(\partial K_T/\partial P)_T$ | 4[f] | 4[f] |
| $(\partial K_T/\partial T)_P$/GPa K$^{-1}$ | 0[f] | 0[f] |
| $\alpha(T) = \alpha_0 + \alpha_1 T + \alpha_2 T^{-2}$ K$^{-1}$ ($T$ in K) | | |
| $\alpha_0 \times 10^5$ | 3.2239[g] | 3.2239[g] |
| $\alpha_1 \times 10^9$ | 2.0[g] | 2.0[g] |
| $\alpha_2$ | 0[g] | 0[g] |

[a] Estimated value, see text
[b] Determined from Raman spectra
[c] Irifune et al. (1991)
[d] Akaogi et al. (1999)
[e] Yutani et al. (1997)
[f] Assumed value
[g] Assumed to be the same as that of $CaFe_2O_4$ calcium ferrite by Skinner (1966)

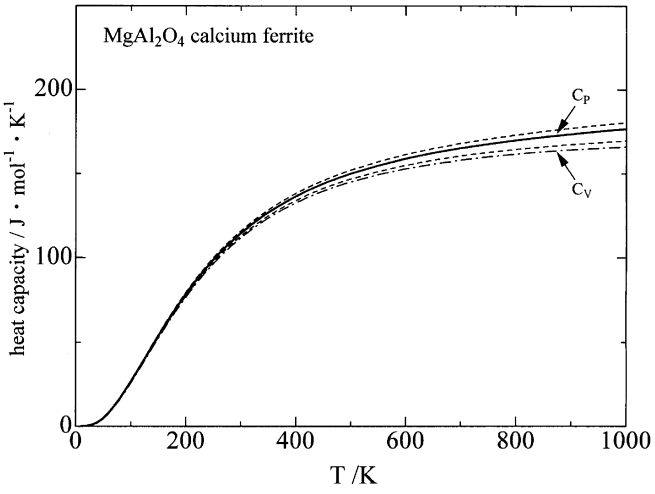


**Fig. 4** Calculated heat capacities of $MgAl_2O_4$ calcium ferrite. *Solid and dash-dotted lines* represent heat capacity at constant pressure ($C_P$) and at constant volume ($C_V$), respectively. *Dashed curves* show the effect of thermal expansivity on the calculated heat capacity. *Upper and lower dashed curves* represent the results of $C_P$ calculations with thermal expansivities of $4 \times 10^{-5}$ K$^{-1}$ and $2 \times 10^{-5}$ K$^{-1}$, respectively

**Table 5** Estimated entropies and thermal Debye temperatures for $MgAl_2O_4$ and $CaAl_2O_4$ calcium ferrites

| | $MgAl_2O_4$ | $CaAl_2O_4$ |
|---|---|---|
| $S^\circ_{298}$/J mol$^{-1}$ K$^{-1}$ | 97.6 | 114.9 |
| $\theta_{D,\,298}$/K | 933 | 831 |

Table 5 together with thermal Debye temperatures obtained at 298 K.

The observation in this study that $MgAl_2O_4$ calcium ferrite was synthesized at higher temperature in the recovered sample than the $Al_2O_3$ + MgO phase suggests that the transition boundary from $Al_2O_3$ + MgO to $MgAl_2O_4$ calcium ferrite has a negative Clapeyron slope. This is consistent with the results of Akaogi et al. (1999) and Irifune et al. (2002). The negative slope indicates that $MgAl_2O_4$ calcium ferrite has a larger entropy than that of $Al_2O_3$ + MgO at high pressures and high temperatures. Actually, the obtained $S^\circ_{298}$ of $MgAl_2O_4$ calcium ferrite, 97.6 J mol$^{-1}$ K$^{-1}$ is larger than the summation of $S^\circ_{298}$ of $Al_2O_3$ (50.9 J mol$^{-1}$ K$^{-1}$) and MgO (26.9 J mol$^{-1}$ K$^{-1}$) by Robie and Hemingway (1995), and the relation does not change up to at least 1500 K using the $C_P$ equation in Table 3 for $MgAl_2O_4$ calcium ferrite and those for $Al_2O_3$ and MgO by Berman (1988). The Clapeyron slope calculated by using the estimated entropy of $MgAl_2O_4$ calcium ferrite was obtained as $\Delta S^\circ_{298}/\Delta V_0 = -0.027$ GPa K$^{-1}$, where volumes of $Al_2O_3$ and MgO from Robie and Hemingway (1995) and of $MgAl_2O_4$ calcium ferrite by Irifune et al. (1991) were used, and the independence of $\Delta S$ and $\Delta V$ of both pressure and temperature was assumed. The calculated slope is relatively steeper than that given in Akaogi et al. (1999) (about −0.003 GPa K$^{-1}$) and Irifune et al. (2002) (about −0.002 GPa K$^{-1}$). This difference may suggest that the above assumption is too simple. However, further, detailed investigation will also be needed to constrain the stability field of $MgAl_2O_4$ calcium ferrite phase under lower mantle conditions.

**Acknowledgements** We thank anonymous reviewers for helpful suggestions and Professor M. Matsui for helping WMIN calculation. This study was supported in part by grants-in-aid from the Ministry of Education, Science and Culture, Japan, and the Japan Society for the Promotion of Science.

## References

Akaogi M, Ross NL, McMillan P, Navrotsky A (1984) The $Mg_2SiO_4$ polymorphs (olivine, modified spinel and spinel)-thermodynamic properties from oxide melt solution calorimetry, phase relations and models of lattice vibrations. Am Mineral 69: 499–512

Akaogi M, Yusa H, Ito E, Yagi T, Suito K, Iiyama JT (1990) The $ZnSiO_3$ clinopyroxene–ilmenite transition: heat capacity, enthalpy of transition and phase equilibria. Phys Chem Miner 17: 17–23

Akaogi M, Hamada Y, Suzuki T, Kobayashi M, Okada M (1999) High pressure transitions in the system $MgAl_2O_4$–$CaAl_2O_4$: a

new hexagonal aluminous phase with implication for the lower mantle. Phys Earth Planet Inter 115: 67–77
Anderson DL, Anderson OL (1970) The bulk modulus–volume relationship for oxides. J Geophys Res 75: 3494–3500
Berman RG (1988) Internally-consistent thermodynamic data for minerals in the system $Na_2O$–$K_2O$–CaO–MgO–FeO–$Fe_2O_3$–$Al_2O_3$–$SiO_2$–$TiO_2$–$H_2O$–$CO_2$. J Petrol 29: 445–522
Berman RG, Brown TH (1985) The heat capacity of minerals in the system $Na_2O$-$K_2O$–CaO–MgO–FeO–$Fe_2O_3$–$Al_2O_3$–$SiO_2$–$TiO_2$–$H_2O$–$CO_2$: representation, estimation, and high temperature extrapolation. Contr Miner Petrol 89: 168–183
Birch F (1961) The velocity of compressional waves in rocks to 10 kilobars, part 2. J Geophys Res 66: 2199–2224
Busing WR (1981) WMIN, a computer program to model molecules and crystals in terms of potential energy functions, report ORNL-5747. Oak Ridge National Laboratory, Tennessee
Hirose K, Fei Y, Ma Y, Mao H (1999) The fate of subducted basaltic crust in the Earth's lower mantle. Nature 397: 53–56
Hofmeister AM (1987) Single-crystal absorption and reflection infrared spectroscopy of forsterite and fayalite. Phys Chem Miner 14: 499–513
Irifune T, Ringwood AE (1993) Phase transformations in subducted oceanic crust and buoyancy relationships at depths of 600–800 km in the mantle. Earth Planet Sci Lett 117: 101–110
Irifune T, Fujino K, Ohtani E (1991) A new high-pressure form of $MgAl_2O_4$. Nature 349: 409–411
Irifune T, Naka H, Sanehira T, Inoue T, Funakoshi K (2002) In situ X-ray observations of phase transitions in $MgAl_2O_4$ spinel to 40 GPa using multianvil apparatus with sintered diamond anvils. Phys Chem Miner 29: 645–654
Kesson SE, Fitz Gerald JD, Shelley JMG (1994) Mineral chemistry and density of subducted basaltic crust at lower-mantle pressures. Nature 372: 767–769
Kieffer SW (1979a) Thermodynamics and lattice vibrations of minerals:1. Mineral heat capacities and their relationships to simple lattice vibrational models. Rev Geophys Space Phys 17: 1–19
Kieffer SW (1979b) Thermodynamics and lattice vibrations of minerals:2. Vibrational characteristics of silicates. Rev Geophys Space Phys 17: 20–34
Kieffer SW (1979c) Thermodynamics and lattice vibrations of minerals: 3. Lattice dynamics and an approximation for minerals with application to simple substances and framework silicates. Rev Geophys Space Phys 17: 35–59
Kieffer SW (1980) Thermodynamics and lattice vibrations of minerals: 4. Application to chain and sheet silicates and orthosilicates. Rev Geophys Space Phys 18: 862–886
Kubo A, Akaogi M (2000) Post-garnet transitions in the system $Mg_4Si_4O_{12}$–$Mg_3Al_2Si_3O_{12}$ up to 28 GPa: phase relations of garnet, ilmenite and perovskite. Phys Earth Planet Inter 121: 85–102
Matsui M (1994) A transferable interatomic potential model for crystals and melts in the system CaO–MgO–$Al_2O_3$–$SiO_2$. Mineral Mag 58A: 571–572
Miyajima N, Yagi T, Hirose K, Kondo T, Fujino K, Miura H (2001) Potential host phase of aluminum and potassium in the Earth's lower mantle. Am Mineral 86: 740–746
Ono S, Ito E, Katsura T (2001) Mineralogy of subducted basaltic crust (MORB) from 25 to 37 GPa, and chemical heterogeneity of the lower mantle. Earth Planet Sci Lett 190: 57–63
Reid AF, Ringwood AE (1969) Newly observed high pressure transformations in $Mn_3O_4$, $CaAl_2O_4$, and $ZrSiO_4$. Earth Planet Sci Lett 6: 205–208
Reid AF, Wadsley AD, Sienko MJ (1968) Crystal chemistry of sodium scandium titanate, $NaScTiO_4$, and its isomorphs. Inorg Chem 7: 112–118
Robie R, Hemingway BS (1995) Thermodynamic properties of minerals and related substances at 298.15 K and 1 bar ($10^5$ Pascals) pressure and at higher temperatures. US Geol Surv Bull 2131
Ross NL, Akaogi M, Navrotsky A, Susaki J, McMillan P (1986) Phase transitions among the $CaGeO_3$ polymorphs (wollastonite, garnet, and perovskite structures): studies by high-pressure synthesis, high-temperature calorimetry, and vibrational spectroscopy and calculation. J Geophys Res 91: 4685–4696
Skinner BJ (1966) Thermal expansion. In: Clark SP, Jr (ed) Handbook of physical constants, Geological Society of America Memoir 97, pp 78–96
Yutani M, Yagi T, Yusa H, Irifune T (1997) Compressibility of calcium ferrite-type $MgAl_2O_4$. Phys Chem Miner 24: 340–344